ISSN: 2836-8495

Research Article

Journal of Current Trends in Computer Science Research

Process of Image Super-Resolution

Sebastien Lablanche[1]*and Gerard Lablanche[2]

[1]*Universite Paul Sabatier Toulouse III, Route de Narbonne, France.*

[2]*Universite de Bordeaux, 351 Cours de la Liberation, France.*

***Corresponding Author**

Sebastien Lablanche, Universite Paul Sabatier Toulouse III, Route de Narbonne, France.

Submitted: 2023, Apr 20 ; **Accepted:** 2023, May 22 ; **Published:** 2023, June 05

Citation: Lablanche, S., Lablanche, G. (2023). Process of Image Super-Resolution. *J Curr Trends Comp Sci Res, 2*(2),108-118.

Abstract

In this paper, we explain a process of super-resolution reconstruction allowing to increase the resolution of an image. The need for high-resolution digital images exists in diverse domains, for example, the medical and spatial domains. The obtaining of high-resolution digital images can be made at the time of the shooting, but it is often synonymic with important costs because of the necessary material to avoid such costs, it is known how to use methods of super-resolution reconstruction, consisting of one or several low-resolution images to obtain a high-resolution image. The American patent US 9208537 describes such an algorithm. A zone of one low-resolution image is isolated and categorized according to the information contained in pixels forming the borders of the zone. The category of it zone determines the type of interpolation used to add pixels in the aforementioned zone, to increase the neatness of the images. It is also known how to reconstruct a low-resolution image and a high-resolution image by using a model of super-resolution reconstruction whose learning is based on networks of neurons and on an image or a picture library. The demand of Chinese patent CN 107563965 and the scientist publication "Pixel Recursive Super Resolution ", R. Dahl, M. Norouzi, and J. Shlens propose such methods. The aim of this paper is to demonstrate that it is possible to reconstruct coherent human faces from very degraded pixelated images with a very fast algorithm, faster than the compressed sensing (CS) algorithm, easier to compute and without deep learning, so without important information technology resources, i.e. a large database of thousand of training images (https://arxiv.org/pdf/2003.13063.pdf). This technological breakthrough has been patented in 2018 with the demand of French patent FR 1855485 (https://patents.google.com/patent/FR3082980A1, see the HAL reference https://hal.archives-ouvertes.fr/hal-01875898v1).

Keywords: Convolutional Neural Networks Emotion Detection Image Processing Music Recommendation

1. Introduction

Last February 2017, three researchers described before from Google Brain published their results on Pixel Recursive Super Resolution to present the powerful IA (https://arxiv.org/pdf/1702.00783.pdf). Their technology consists in approaching the final picture by combining an algorithm and database pictures of Google to obtain from an initial 8x8 definition picture, a 32x32 definition picture which is very similar to the actual picture. A French startup named LABLANCHE (http://www.lablanche-and-co.com) is said to have developed an innovation based on a powerful algorithm that could deliver similar results as Google, but, without using any database. If the achievements of this new algorithm are confirmed, it would represent a very important innovation for any potential end user who would want to operate independently of the Google database, and faster. In this paper, we present the new technology of interpolation for image super-resolution based on conditional interpolations in three directions called successively to achieve a blurred high-resolution image with a lot more details to help the deconvolution algorithm (the directional interpolation monitored by the orientation of the motion filter) to create truth details at the end (LABLANCHE process).

2. Problem

2.1 Presentation

For the tests, we must realize two stages. For stage 1, we do a compression of images which consists to fill in each bloc of 4x4 pixels of R, G, or B channel with an averaging intensity of the bloc. For stage 2, we do storage of intensities in a vector of unsigned char type for the channel (if monochrome image) or three channels (if RGB image). In the C++ language, the unsigned char type elements correspond to bytes. This stage provides a smaller size file that attains averaging intensities. The parameter named step corresponds to the size of the same color blocs, step controls the quality of the reconstruction and therefore the loss of quality generated by the compression. For step=4, the compression rate is equivalent to the JPEG size format (step and step/2 must be even numbers to realize the reconstruction). We note q=step/2, the number of levels. Here we have two levels LEVEL 1 and LEVEL 2 and the step is an even number which enables us to share the 4 by 4 pixels bloc in 4 blocs qxq. In the case of 2 by 2 pixels blocs, we have one level (step=2).

2.2 Modelling

Considering that images as vectors, the problem can be modeled with a lower solution observation named *B* of the original image I which is obtained by applying an operator of movement *M* (i.e. a geometric transformation), a blur operator *F*, and with a subsampling operator *S*. An additive noise completes this inverse problem: *B=SFMI+*. The operator *SFM* (subsampling + blurring + geometric transformation) owns more columns than rows, the system is underdetermined. The extension factor between images *B* and the e *I* is equal to step².The image *H* obtained by a super-resolution algorithm from *B* must be verified the reconstruction constraint, i.e. must give *B* using the observation model.

3.Compressed Sensing

The Compressed Sensing technique makes it possible to find the most parsimonious solution from an undetermined linear system. It involves not only the means of finding such a solution but also the linear systems that are acceptable. The process is to reconstruct accurately a signal or an image when the number of measurements is less than the length of the signal. The paradox can be explained by the fact that the signal admits a sparse representation on an appropriate basis. This sampling aims to replace the classic Shannon sampling. This theory has been widely developed in recent years and the amount of applications is continuing to rise in diverse fields such as tomography with MRI and computed tomography or radar and radar imagery, in particular in signal and image compression. We consider a real-valued signal *x*, which we will see in the form of a column vector of length N. In the case of images or higher-dimension signals, we can arrange the data to form a long vector. We indicate this signal in a Ψ base such as $x=\Psi s$. We wish to select the base whereby the majority of coefficients of s are equal to zero, ie *x* is parsimonious in the base Ψ.

These bases are known and usually used to compress the starting signal. Compressed Sensing proposes to acquire directly the compressed version of the signal so that unnecessary samples do not need to be processed. The linear measuring process that is used consists of making M scalar products, with M much smaller than N, between *x* and a collection of vectors going from 1 to M. We obtain therefore samples $y_j = \langle x, \Phi_j \rangle$of measurements. Considering that the measurement matrix Φ has the (Φj) as a column, we can thus write *x* as $y = \Phi x = \Phi\Psi s = \Theta s$ (with $\Theta = \Phi\Psi$). The measurement matrix design must be able to find the most parsimonious signals. In order to do so, the measurement matrix must follow certain properties, one of which is called RIP (Restricted Isometry Property). The matrix Φ satisfies the restricted isometry property (RIP) of order k if there exists δ_k in (0,1) such that $(1\text{-}\delta_k)\|x\|_2^2 \leq \|\Phi x\|_2^2 \leq (1+\delta_k)\|x\|_2^2$ holds for all $x \in \Sigma_k = \{x : \|x\|_0 \leq k\}$. Furthermore, must be inconsistent with, Ψ so the coherence of the Θ matrix must be closest to 0. The coherence μ of a matrix Θ is the largest absolute inner product between any two columns of Θ and is defined by $\mu(\Theta) = \max_{1 \leq i \leq j \leq n} \frac{\langle \Theta_i, \Theta_j \rangle}{\|\Theta_i\| \|\Theta_j\|}$.
It is evident that these properties are satisfied with a high probability simply by choosing Φ at random, for example by using a Gaussian distribution. Although these RIP or inconsistency conditions are satisfactory for some sets of measurements, they are only necessary conditions and not sufficient. There are other properties, also insufficient, which require us to need even fewer samples in order to guarantee a parsimonious signal reconstruction. The last step of the Compressed Sensing process is the reconstruction of the starting signal. For this, we know the M values for y, the matrix measurements used as well as the Ψ base.

These bases are known and usually used to compress the starting signal. Compressed Sensing proposes to acquire directly the compressed version of the signal so that unnecessary samples do not need to be processed. The linear measuring process that is used consists of making M scalar products, with M much smaller than N, between x and a collection of vectors going from 1 to M. We obtain therefore samples of measurements. Considering that the measurement matrix _ has the as a column, we can thus write The measurement matrix design must be able to find the most parsimonious signals. In order to do so, the measurement matrix must follow certain properties, one of which is called RIP (Restricted Isometry Property). The matrix satisfies the restricted isometry property (RIP) of order k if there exists Furthermore, must be inconsistent with, so the coherence of the matrix must be closest to 0. The coherence μ of a matrix is the largest absolute inner product between any two columns of and is defined by It is evident that these properties are satisfied with a high probability simply by choosing at random, for example by using a Gaussian distribution. Although these RIP or inconsistency conditions are satisfactory for some sets of measurements, they are only necessary conditions and not sufficient. There are other properties, also insufficient, which require us to need even fewer samples in order to guarantee a parsimonious signal reconstruction. The last step of the Compressed Sensing process is the reconstruction of the starting signal. For this, we know the M values for y, the matrix measurements used as well as the base.

The reconstruction algorithm seeks to find the coefficients of s. Thanks to this knowledge, it is then simple to find x, the starting signal. There are infinite solutions for the equation s=y, however, we are looking for the solution which minimizes a certain norm. The L2 norm measures the signal energy which is why by using a L2-Minimization, we will hardly ever find a K-parsimonious result. The L0 norm measures the parsimony of the signal (we count the number of elements not equal to zero), and the optimization $\hat{s} = \arg\min \|s\|_0$ such as $\Theta s = y$ gives a good result (L0-Minimization). The disadvantage is that this problem cannot be calculated digitally. It has been shown that the optimization based on the L1 norm makes it possible to find an exact K-parsimonious signal, the problem of the L1-Minimization is convex. Its resolution could be reduced to a linear program, more often known as basis pursuit. This resolution is not the only one and there are other techniques that allow for even better results such as Conjugate Gradient Pursuit (CGP) or Stage-wise Weak Conjugate Gradient Pursuit (StWCGP). The number of necessary measurements M to have an exact recovery of the K-parsimonious signal is in the same order as 5K.

4. Model

We use a reconstruction of the pixelated image with an algorithm of conditional and directional interpolation. The algorithm owns as its scientific base the fact when the ratio of the pixels is very small the decoherence used in compressed sensing (CS) plays an important role in the quality of reconstruction whereas parsimony plays an important role when the ratio is more

important (over 10%). So, the parsimony research is efficient for the problem with step=2 but is inefficient for step=4 and step=3. The algorithm mixes the information in order to approach reality because the decoherence is controlled by following conditional interpolations in three possible directions which enables the deconvolution (the final step called directional interpolation) to create the details to give an acceptable reconstruction.

4.1 Conditional Interpolation

We start with a 4x4 pixels bloc filled in with an averaging intensity (B bloc). The B block is divided into four similar neighbors 2x2 blocs: B1, B2, B3, and B4. The B1 bloc (at the top and on the left) always keeps its starting intensity. The B bloc (4x4) owns three 4 by 4 neighbors blocs C, D, and, E, and data interpolation is controlled by three parameters p2, p3, and p4:

a) The C bloc (on the right)
b) The D bloc (at the bottom)
c) The E bloc (at the bottom and on the right).
d) p2 is the parameter that controls the mean between the B bloc and the C bloc
e) p3 is the parameter that controls the mean between the B bloc and the D bloc
f) p4 is the parameter that controls the mean between the B bloc and the E bloc.

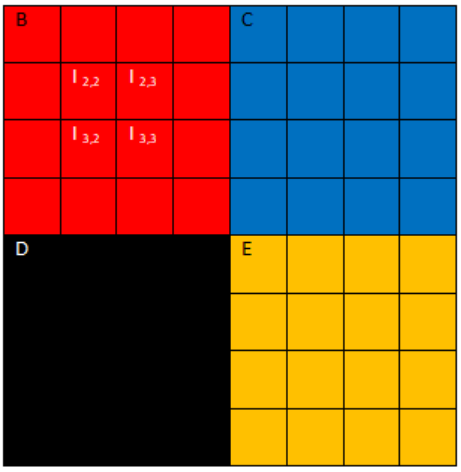

Figure 1: illustration of the image splitting in four neighbor blocs B,C,D,E.

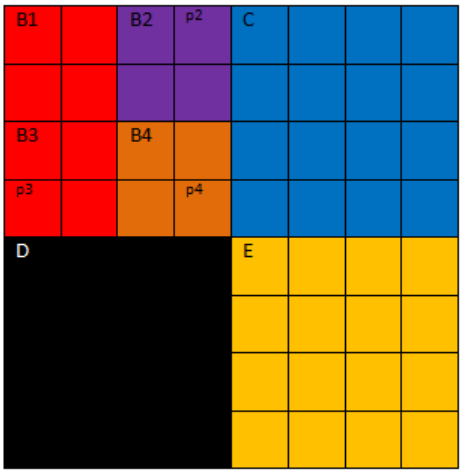

Figure 2: illustration of LEVEL 1 interpolation.

i. B1 keeps the color of B bloc (always)
B2 takes the average color $\frac{(B+C)}{2}$ if $|B-C| \leq p2$ and keeps the B color otherwise
ii. B3 takes the average color $\frac{(B+D)}{2}$ if $|B-D| \leq p3$ and keeps the B color otherwise
iii. B4 takes the average color $\frac{(B+E)}{2}$ if $|B-E| \leq p4$ and keeps the B color otherwise.

The setting of the p2, p3, and p4 parameters is very important. We realize the interpolation between the two blocs only if they have enough closed colors. These parameters are integers between 0 and 255. If the value is equal to 0, there is no interpolation and if the value is 255, the interpolation is always realized. In other cases, the interpolation is realized if the two adjacent blocs have intensities with a smaller difference than the constraint. The goal of this step is to separate different interest areas of the image and to generate contrast enhancement. We called the LEVEL 1 routine several times with different parameters p2, p3, and p4 to obtain the contrast enhancement, t, and the last call is realized with non-conditional interpolations e.g. with p2 = 255, p3 = 255, p4 = 255 in order to have a pre-smoothing. We use the mean of the central square $\frac{I_{2,2}+I_{2,3}+I_{3,2}+I_{3,}}{4}$ to colorize the 4 by 4 pixels bloc in Figures 1 and 2. In this example, the B2 bloc and the B4 bloc are changed by interpolation and the B3 bloc keeps its color because of the constraints. We start with the B1 bloc which is divided into 4 neighbors blocs of size 1 (pixels): B11, B12, B13, and B14, the B11 pixel (at the top and on the left) always keeps the B1 bloc intensity (Figure 3).

iv. B11 keeps the color of B1 bloc (always)
v. B12 takes the average color $\frac{(B1+B2)}{2}$ if $|B1-B2| \leq p2$ and keeps the B1 color otherwise
vi. B13 takes the average color $\frac{(B1+B3)}{2}$ if $|B1-B3| \leq p3$ and keeps the B1 color otherwise
vii. B14 takes the average color $\frac{(B1+B4)}{2}$ if $|B1-B4| \leq p4$ and keeps the B1 color otherwise
viii. p2' is the parameter that controls the mean between the B1 bloc and the B2 bloc
ix. p3' is the parameter that controls the mean between the B1 bloc and the B3 bloc
x. p4' is the parameter that controls the mean between the B1 bloc and the B4 bloc.

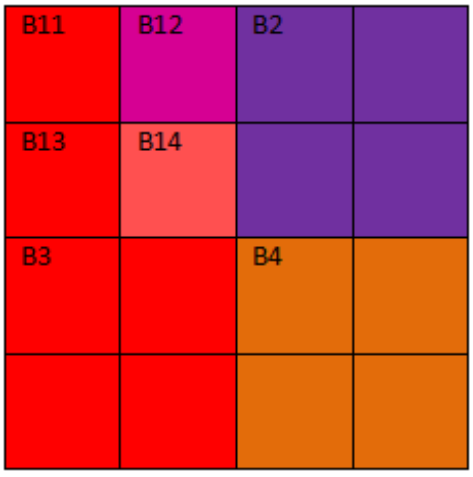

Figure 3: illustration of LEVEL 2 interpolation.

4.2 Directional Interpolation

The deconvolution with the motion blur filter aims to create details of the image. The deconvolution can be formulated by the inverse problem y =hⒶx where h is the motion blur filter, y is the observed image, x is the unknown image and Ⓐ is the convolution operator. The idea is to increase the size of the filter until the details are created but it is possible only with a well-designed y image built using the appropriate conditional interpolations. The motion filter owns two parameters, the distance L and the direction θ (or the angle of deconvolution). Before the deconvolution, n we must increase the size of the image with a magnification factor γ to avoid the creation of blurred blocs on the image after the deconvolution. In practice, γ depends of the geometry of the image (Tables 2 and 3). The parameters of conditional interpolations are known after a step of deep learning with a large database of HR and LR images and the better values are chosen to obtain the better interpolation, much less blurred than the other interpolation methods such as bicubic interpolations. The range of values for the parameter L begins from 0 to 19 and the range of values begins from 0 to 170 by step of 5 degrees. For an image, there is a resonance angle (by analogy with the resonance frequency) which appears when the user makes the motion deconvolution algorithm because the details are created only with this value of θ. We note θˆ this unique value. The length parameter L depends of the size of the image, its value decreases when the size of the image is larger. This phenomenon leads us to build a new mathematical theory where the structure of images will be described with an angle of movement instead of a wavelet. The information can be represented as a matrix with different calls of LEVEL 1 interpolations. In practice, we need only three or four LEVEL 1 interpolations, the first has the role of contrast enhancement and the two last correspond to the pre-smoothing. The smoothing has two components: the last call of LEVEL 1 interpolation just after the different areas are dissociated and the LEVEL 2 interpolation at the end of the interpolation process. We write the three parameters of the first LEVEL 1 occurrence $p2^{(1)}$, $p3^{(1)}$, $p4^{(1)}$. For the second occurrence $p2^{(2)}$, $p3^{(2)}$, $p4^{(2)}$, and for the third occurrence $p2^{(3)}$, $p3^{(3)}$, $p4^{(3)}$ (the fourth occurrence $p2^{(4)}$, $p3^{(4)}$, $p4^{(4)}$ is optional). There are three deconvolutions, the first $\gamma^{(1)}$, $L^{(1)}$, $\theta^{\gamma(1)}$ is the more important to approach the right geometry, and the two others aim to

$$\text{LABLANCHE}=\begin{pmatrix} p2^{(1)} & p3^{(1)} & p4^{(1)} \\ 255 & 255 & 255 \\ \gamma^{(1)} & L^{(1)} & \hat{\theta^{(1)}} \\ Source^{(1)} & Amount^{(1)} & Noise^{(1)} \\ p2^{(2)} & p3^{(2)} & p4^{(2)} \\ 255 & 255 & 255 \\ 1 & L^{(2)} & \hat{\theta^{(2)}} \\ Source^{(2)} & Amount^{(2)} & Noise^{(2)} \\ p2^{(3)} & p3^{(3)} & p4^{(3)} \\ 255 & 255 & 255 \\ 1 & L^{(3)} & \hat{\theta^{(3)}} \\ Source^{(3)} & Amount^{(3)} & Noise^{(3)} \\ p2^{(4)} & p3^{(4)} & p4^{(4)} \\ 255 & 255 & 255 \\ 255 & 255 & 255 \end{pmatrix} \quad (1)$$

The source is the source image (DVC: Digital Video Camera or OFC: Old Film Camera), *Amount* (to apply to the image) (100, 125, 150, 200, 250, or 300 %) and Noise the choice Remove noise (Yes/No or DO: Dark Only or LO: Light Only).

We indicate the motion blur filter h for L=13 and θ=105◦ (13 columns and 5 rows matrix) which is optimal for Marie Bonneau (Figure 4).

$$h=\begin{pmatrix} 0.0384 & 0.0310 & 0 & 0 & 0 \\ 0.0273 & 0.0507 & 0 & 0 & 0 \\ 0.0078 & 0.0703 & 0 & 0 & 0 \\ 0 & 0.0612 & 0.0169 & 0 & 0 \\ 0 & 0.0416 & 0.0364 & 0 & 0 \\ 0 & 0.0221 & 0.0560 & 0 & 0 \\ 0 & 0.0026 & 0.0755 & 0.0026 & 0 \\ 0 & 0 & 0.0560 & 0.0221 & 0 \\ 0 & 0 & 0.0364 & 0.0416 & 0 \\ 0 & 0 & 0.0169 & 0.0612 & 0 \\ 0 & 0 & 0 & 0.0703 & 0.0078 \\ 0 & 0 & 0 & 0.0507 & 0.0273 \\ 0 & 0 & 0 & 0.0310 & 0.0384 \end{pmatrix} \quad (2)$$

h is a vector for horizontal and vertical direction and a matrix otherwise. The filter *h* plays the role of the matrix Ψ in the parsimonious research (Compressed Sensing section). The columns are symmetrical to the central column, but they are reversed.

L \ θ	5°	15°	25°	35°	45°	55°	65°	75°	85°	95°	105° ...
0	×	×	×	×	×	×	×	×	×	×	×
1	×	×	×	×	×	×	×	×	×	×	×
2	×	×	×	×	×	×	×	×	×	×	×
3	×	×	×	$(L^3, \hat{\theta}^3)$	×	×	×	×	×	×	×
4	×	×	×	×	×	×	×	×	×	×	×
5	$(L^2, \hat{\theta}^2)$	×	×	×	×	×	×	×	×	×	×
6	×	×	×	×	×	×	×	×	×	×	×
7	×	×	×	×	×	×	×	×	×	×	×
8	×	×	×	×	×	×	×	×	×	×	×
9	×	×	×	×	×	×	×	×	×	×	×
10	×	×	×	×	×	×	×	×	×	×	×
11	×	×	×	×	×	×	×	×	×	×	×
12	×	×	×	×	×	×	×	×	×	×	×
13	×	×	×	×	×	×	×	×	×	×	$(L^1, \hat{\theta}^1)$
14	×	×	×	×	×	×	×	×	×	×	×
15	×	×	×	×	×	×	×	×	×	×	×
16	×	×	×	×	×	×	×	×	×	×	×
17	×	×	×	×	×	×	×	×	×	×	×

Figure 4: motion deconvolution grid, (L, θ^) is optimal for Marie Bonneau.

5. Experiments

In the case where step and q are not even numbers, for example for step=3, we define q=E(step/2) where E is the integer part. The B1 bloc is a 2 by 2 pixels bloc but the sizes of B2, B3, and B4 are different. The B2 bloc is a 2 by 1 pixels bloc, the B3 bloc is a 1 by 2 pixels bloc and the B4 bloc is a pixel. The B2 bloc is stretched in the direction of the right adjacent bloc and the B3 bloc is stretched in the direction of the bottom adjacent bloc which enables us to say that the geometry of this interpolation method is optimal for the case where step=3 (Figure 5).

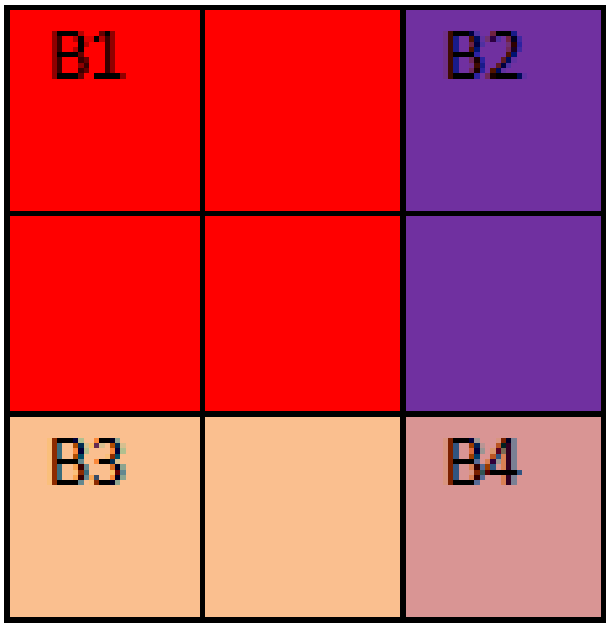

Figure 5: Illustration of the case 3 by 3 pixels.

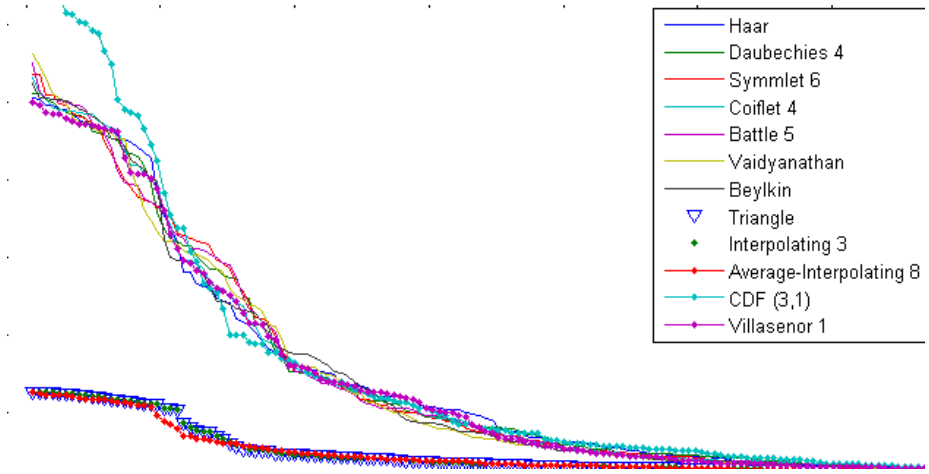

Figure 6: Comparison of the decreases of the different wavelet family's coefficients in absolute value (Marie Bonneau image), the largest Villasenor coefficients (purple dot curve) are lower than for other wavelet families and their decay is faster (smallest L1 norm). The interpolation wavelets' magnitudes (Triangle, Interpolating, Average-Interpolating) are much lower but are suitable only for 50% of randomly known pixels using L1-minimization (Figure 10). The decay of the CDF wavelet family is the fastest but the magnitude of larger CDF coefficients is higher than for the other wavelet families. We observed the same curves for all images.

The algorithm described before is the same with these new B2, B3, and B4 blocs and the L parameter is smaller because we need a weaker deconvolution than the deconvolution used in the case of 4 by 4 pixels. The angle of resonance θ is the same for a given image. This case is important because it corresponds to 11 % of known pixels and we demonstrate that the 11 % larger coefficients approximation in the best wavelet base (in general Villasenor 1 or Villasenor 5) is very precise for visual identification by the human eye (the starry image on Figure 7). Unfortunately, this algorithm gives catastrophic results, so we can present only the case 4 by 4 pixels. We have an equivalence between the pixel's ratio and the best wavelet larger coefficients kept ratio in the quality of reconstruction and approximation. Villasenor 1 is the wavelet basis used in the JPEG 2000 standard. The best wavelets are Villasenor 1,2,3,4,5 (Figure 6). The optimal wavelet for Marie Bonneau is Villasenor 5 (Figures 7,8 and Table 1). The interest of our algorithm will be to obtain similar quality reconstructions from 8x8 low-resolution images in comparison with 11% larger coefficients kept approximations in the optimal wavelet basis (Figures 9,10).

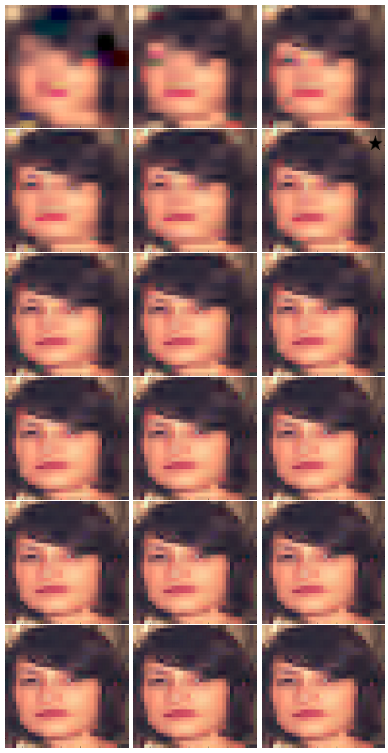

Figure 7: Approximation of Marie Bonneau with 6,7,8% (First line), 9,10,11% (Second line), 12,13,14% (Third line), 15,16,17% (Fourth line), 18,19,20%(Fifth line), 21,22,23%(Sixth line) of larger coefficients in Villasenor 5 wavelet basis.

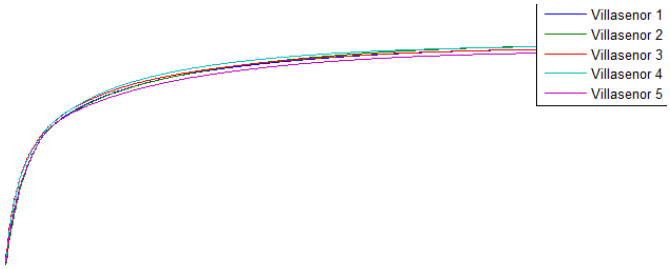

Figure 8: cumulative sums of the coefficients in absolute values of the Villasenor wavelets for Marie Bonneau (1) (illustrating technology image), the lower magnitude is the purple curve.

Part	
Name 32x32	optimal wavelet
Google Brain (1)	Villasenor 1
Google Brain (2)	Villasenor 5
Google Brain (3)	Villasenor 1
Marie Bonneau (1)	Villasenor 5
Marie Bonneau (2)	Villasenor 1
Ellie Goulding	Villasenor 1
Ariana Grande	Villasenor 5
Shailene Woodley	Villasenor 5
Man	Villasenor 1
Eye	Villasenor 1
Meghan Markle	Villasenor 5

Table 1: table of test images.

We use eleven test images of 32x32 pixels for our algorithm: Google Brain (3 images), Marie Bonneau (2 images), Ellie Goulding, Ariana Grande, Man, Shailene Woodley, Ronald Coifman (eye), and Meghan Markle. We give the optimal wavelet for each of the eleven test images (Table 1) and the directional and conditional interpolations parameters obtained after tests on a large dataset of images with different geometries. We have chosen one of the best combinations of parameters that bring out the resonance angle of motion deconvolution following the scheme described below (Figure 9), the magnification factor is learned and known for each image (Tables 2 and 3).

$i \leftarrow 1$;
$treshold \leftarrow value$;
Inputs: $\mathcal{I}$, $\mathcal{H}$, $treshold$
while $\|\mathcal{I} - \mathcal{H}\|_2^2 + \lambda\mathcal{R}(\mathcal{H}) \geq treshold$ **do**
  $\hat{\mathcal{H}} \leftarrow \underset{p2^{(i)},p3^{(i)},p4^{(i)},L^{(i)},\theta^{(i)},Source^{(i)},Amount^{(i)},Noise^{(i)}}{\arg\min} \|\mathcal{I} - \mathcal{H}\|_2^2 + \lambda\mathcal{R}(\mathcal{H})$;
  $p2^{(i)} \leftarrow \hat{p2^{(i)}}$;
  $p3^{(i)} \leftarrow \hat{p3^{(i)}}$;
  $p4^{(i)} \leftarrow \hat{p4^{(i)}}$;
  $L^{(i)} \leftarrow \hat{L^{(i)}}$;
  $\theta^{(i)} \leftarrow \hat{\theta^{(i)}}$;
  $Source^{(i)} \leftarrow \hat{Source^{(i)}}$;
  $Amount^{(i)} \leftarrow \hat{Amount^{(i)}}$;
  $Noise^{(i)} \leftarrow \hat{Noise^{(i)}}$;
  $i \leftarrow i + 1$;
  $\mathcal{H} \leftarrow \hat{\mathcal{H}}$;
end
$\hat{\mathcal{H}} \leftarrow \underset{p2^{(i)},p3^{(i)},p4^{(i)}}{\arg\min} \|\mathcal{I} - \mathcal{H}\|_2^2 + \lambda\mathcal{R}(\mathcal{H})$;
Output: $\hat{\mathcal{H}}$

R is a regulator and is the compromise between the norm minimization and the regularization, I am the original image, $\hat{H}$ is the solution obtained with optimal parameters and H is the 8x8 low-resolution input image. It is known to use total variation minimization, but here we define R as the inverse of the sum of 8x8 windows contrasts of the image because on the one hand, the aim of these constraints is to enhance the contrast and on the other hand the contrast of pixels is low inside a 4x4 window but is very high in an 8x8 window (close to 1). For a 32x32 image, there are 16 windows of 8 by 8 pixels and $\mathcal{R}=\frac{1}{\sum_{i=1}^{16} C_i}$

Where C_i is the contrast of the i^{th} block defined by $\frac{I_{max}-I_{min}}{I_{max}+I_{min}}$

(I_{max} and I_{min} are the maxima and the minimum intensity of the i^{th} bloc).

Part		
Name 32x32	conditional interpolation parameters (Right image)	γ
Google Brain (1)	$p2^{(1)}$=63, $p3^{(1)}$=255, $p4^{(1)}$=20	3.80
Google Brain (2)	$p2^{(1)}$=65, $p3^{(1)}$=0, $p4^{(1)}$=65	3.40
Google Brain (3)	$p2^{(1)}$=195, $p3^{(1)}$=0, $p4^{(1)}$=0	3.62
Marie Bonneau (1)	$p2^{(1)}$=135, $p3^{(1)}$=10, $p4^{(1)}$=20	2.25
Marie Bonneau (2)	$p2^{(1)}$=88, $p3^{(1)}$=70, $p4^{(1)}$=0	2.25
Ellie Goulding	$p2^{(1)}$=85, $p3^{(1)}$=55, $p4^{(1)}$=0	2.20
Ariana Grande	$p2^{(1)}$=50, $p3^{(1)}$=225, $p4^{(1)}$=0	3.83
Shailene Woodley	$p2^{(1)}$=75, $p3^{(1)}$=0, $p4^{(1)}$=0	3.05
Man	$p2^{(1)}$=90, $p3^{(1)}$=98, $p4^{(1)}$=0	3.20
Eye	$p2^{(1)}$=105, $p3^{(1)}$=110, $p4^{(1)}$=0	2.05
Meghan Markle	$p2^{(1)}$=98, $p3^{(1)}$=60, $p4^{(1)}$=0	2.25

Table 2: table of results (interpolation).

Part		
Name 32x32	deconvolution parameters (Right image)	γ
Google Brain (1)	L=16, θ=90°; L=7, θ=45°; L=15, θ=75°;	3.80
Google Brain (2)	L=15, θ=70°; L=6, θ=150°;	3.40
Google Brain (3)	L=17, θ=115°;	3.62
Marie Bonneau (1)	L=13, θ=105°; L=5, θ=5°; L=3, θ=35°;	2.25
Marie Bonneau (2)	L=12, θ=160°; L=11, θ=155°; L=2, θ=25°;	2.25
Ellie Goulding	L=11, θ=125°; L=9, θ=10°; L=5, θ=35°;	2.20
Ariana Grande	L=16, θ=100°; L=5, θ=160°; L=5, θ=60°; L=11, θ=35°; L=6, θ=180°;	3.83
Shailene Woodley	L=13, θ=120°; L=6, θ=20°;	3.05
Man	L=20, θ=140°; L=5, θ=120°; L=5, θ=5°;	3.20
Eye	L=10, θ=170°; L=5, θ=25°;	2.05
Meghan Markle	L=11, θ=105°;	2.25

Table 3: table of results (deconvolution).

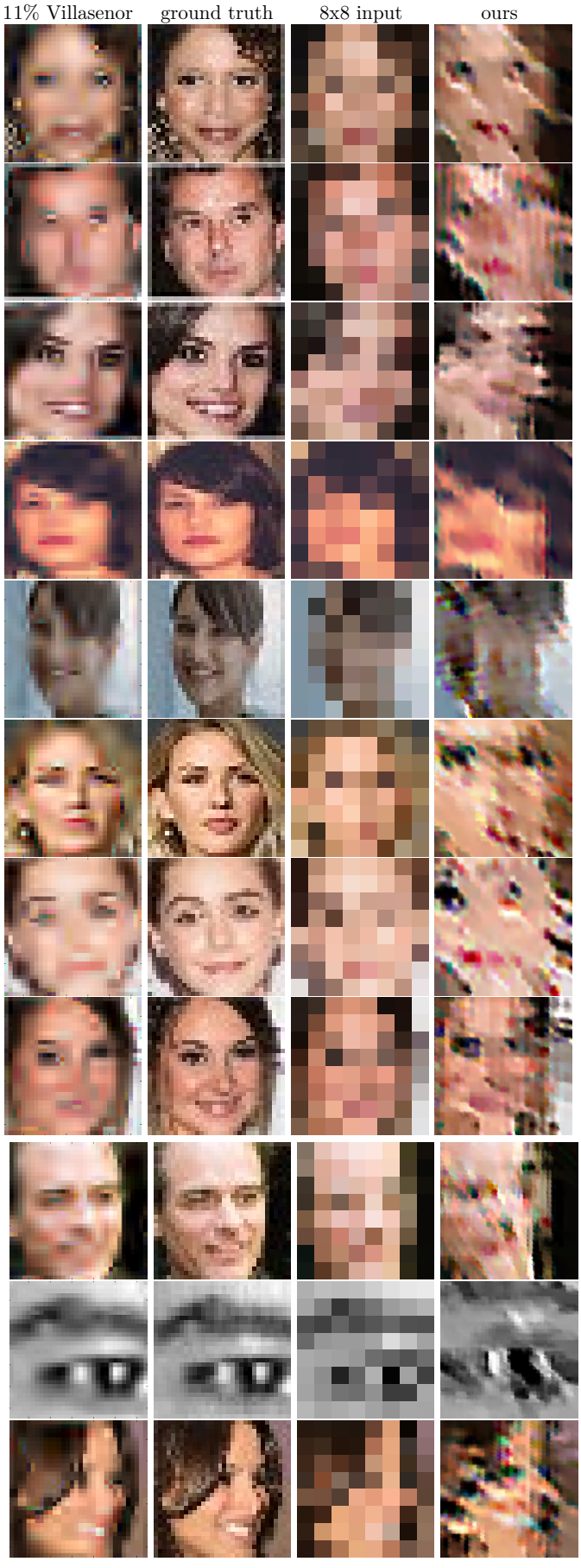

Figure 9: Reconstruction results (Right column) from 8x8 low-resolution images (Middle Right column), 32x32 ground truth images (Middle Left column), and 11% of Villasenor 1/Villasenor 5 larger coefficients approximations (Left column).

We give the complete data results according to the model described before. The deconvolution algorithm is very easy to use and the choice of parameters is easy and fast for the user who can see the different possibilities for the reconstruction. Moreover, the complexity of interpolations is very low because we use only three adjacent blocs (below the Left matrix: Google Brain (1), the Middle matrix: Google Brain (2), and the Right matrix: Marie Bonneau (1)).

$$\begin{pmatrix} 63 & 255 & 20 \\ 255 & 255 & 255 \\ 3.80 & 16 & 90° \\ DVC & LO & 100\% \\ 1 & 7 & 45° \\ DVC & LO & 75\% \\ 1 & 15 & 75° \\ DVC & DO & 0\% \\ 65 & 0 & 65 \\ 255 & 255 & 255 \\ 255 & 255 & 255 \end{pmatrix} ; \begin{pmatrix} 65 & 0 & 65 \\ 255 & 255 & 255 \\ 3.40 & 15 & 70° \\ OFC & YES & 300\% \\ 65 & 0 & 65 \\ 255 & 255 & 255 \\ 1 & 6 & 150° \\ DVC & YES & 75\% \\ 75 & 0 & 0 \\ 255 & 255 & 255 \\ 1 & 6 & 155° \\ DVC & DO & 50\% \\ 75 & 0 & 0 \\ 255 & 255 & 255 \\ 255 & 255 & 255 \end{pmatrix} ; \begin{pmatrix} 135 & 10 & 20 \\ 255 & 255 & 255 \\ 2.25 & 13 & 105° \\ DVC & DO & 100\% \\ 1 & 5 & 5° \\ DVC & LO & 150\% \\ 1 & 3 & 35° \\ DVC & AUTO & 125\% \\ 135 & 10 & 20 \\ 255 & 255 & 255 \\ 255 & 255 & 255 \end{pmatrix} ; \begin{pmatrix} (1), (2), (3) \end{pmatrix}$$

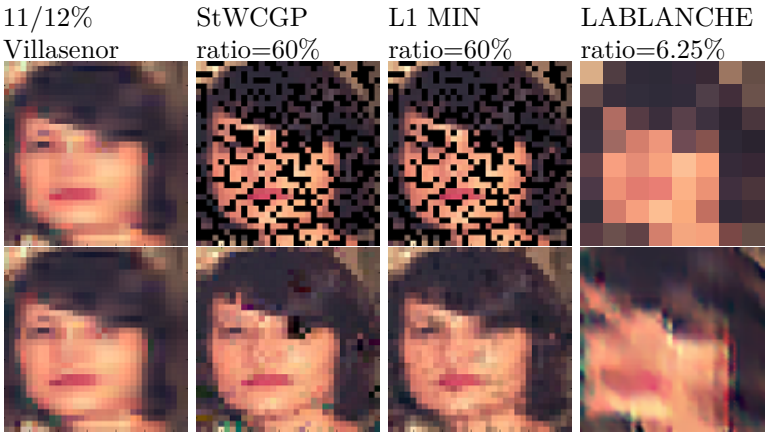

Figure 10: Comparison of the different reconstruction methods. From Left to Right: 11% and 12% of Villasenor 5 larger coefficients approximations (Left column), Stage wise Weak Conjugate Gradient Pursuit (StWCGP) in Villasenor 5 basis from 60% of randomly known pixels (Middle Left column), L1-Minimization in Average-Interpolating 8 basis from 60% of randomly known pixels (Middle Right column) and our method (Right column) from 6.25% of known pixels (8x8 low-resolution input). Our method gives similar quality results to Compressed Sensing from 60% of pixels but with only 6.25% of pixels. Moreover, it is easier to sample the image with a regular grid at the industrial level, therefore our algorithm can represent a new possible technological solution.

6. Conclusion

We have introduced a new class of algorithms based on new interpretations of deconvolution. Motion deconvolution is used to reconstruct details of the image instead of deblurring forensic images. We note that the complexity is low and this process is easy to compute in comparison with deep learning, compressed sensing, a mixture of both, or the categorization of zones. In the future, it would be interesting to find a better deconvolution algorithm and to find a trick to understand the links between conditional interpolations and the optimal angle of deconvolution. The interpretation of these results is to see images as a combination of angles generated by conditional interpolations and the coherence of these angles is achieved with the optimal orientation of the motion deconvolution.

7. Acknowledgments

We thank Jean-Marc Azais (Institute de Mathematiques de Toulouse) and mostly Charles Dossal because his help has been very precious in our work to compute biorthogonal wavelet bases for large-scale problems inside the StWCGP algorithm (inversion of the analysis and synthesis wavelet filters for the calculation of the multiplication by the transposed matrix), without his help, my father couldn't have identified the transfer between the parsimonious research (L1-Minimization and L0-Minimization) and the decoherent research (conditional interpolations) when the information pixels rate decreases.

Of course, I would like to thank my father Gerard LABLANCHE, and my mother Marie-Therèse LABLANCHE.

References

1. Yonina C.Eldar and Gitta Kutyniok. (2012). Compressed Sensing Theory and Applications.
2. Mallat, S. (2000). Une exploration des signaux en ondelettes,

les editions de l‟ ecole polytechnique. Paris, juillet.
3. Dossal, C. H. (2005). Estimation de fonctions geometriques et deconvolution (Doctoral dissertation, Ecole Polytechnique X).
4. Blahut, R. E., Miller, W., & Wilcox, C. H. (1991). Radar and Sonar: Part I (Vol. 32, pp. 1-5). New York: Springer-Verlag.
5. Park, S. C., Park, M. K., & Kang, M. G. (2003). Super-resolution image reconstruction: a technical overview. IEEE signal processing magazine, 20(3), 21-36.
6. Sen, P., & Darabi, S. (2009, November). Compressive image super-resolution. In 2009 Conference Record of the Forty-Third Asilomar Conference on Signals, Systems and Computers (pp. 1235-1242). IEEE.
7. Yang, J., Wright, J., Huang, T. S., & Ma, Y. (2010). Image super-resolution via sparse representation. IEEE transactions on image processing, 19(11), 2861-2873.
8. Elad, M., & Aharon, M. (2006). Image denoising via sparse and redundant representations over learned dictionaries. IEEE Transactions on Image processing, 15(12), 3736-3745.
9. Irani, M., & Peleg, S. (1991). Image sequence enhancement using multiple motions analysis (pp. 216-221). Hebrew University of Jerusalem. Leibniz Center for Research in Computer Science. Department of Computer Science.
10. Wright, J., Yang, A. Y., Ganesh, A., Sastry, S. S., & Ma, Y. (2008). Robust face recognition via sparse representation. IEEE transactions on pattern analysis and machine intelligence, 31(2), 210-227.
11. Chang, H., Yeung, D. Y., & Xiong, Y. (2004, June). Super-resolution through neighbor embedding. In Proceedings of the 2004 IEEE Computer Society Conference on Computer Vision and Pattern Recognition, 2004. CVPR 2004. (Vol. 1, pp. I-I). IEEE.